Medical Engineering and Physics 67 (2019) 78–87

Contents lists available at ScienceDirect

Medical Engineering and Physics

journal homepage: www.elsevier.com/locate/medengphy

In-vitro experimental study of histopathology of bone in vibrational drilling

Khurshid Alam[a,*], Ahmed Al-Ghaithi[b], Sujan Piya[a], Ashraf Saleem[c]

[a] Department of Mechanical and Industrial Engineering, Sultan Qaboos University, P.O. Box 33, Al-Khoud 123, Sultanate of Oman
[b] Orthopaedic Department, Sohar Hospital, Sultanate of Oman
[c] Department of Electrical and Computer Engineering, Sultan Qaboos University, P.O. Box 33, Al-Khoud 123, Sultanate of Oman

ARTICLE INFO

Article history:
Received 29 June 2018
Revised 9 March 2019
Accepted 30 March 2019

Keywords:
Bone drilling
Vibrational drilling
Drilling force
Bone temperature
Bone histology
Statistical analysis

ABSTRACT

Drilling is a common surgical procedure for fracture treatment and reconstruction in multiple surgical fields, including orthopaedics, neurology, and dentistry. Drilling delicate tissue (such as bone) with a hard metallic tool is considered notorious for inducing mechanical and thermal damage, which can adversely affect osseointegration and may weaken the bond between the bone and implant, or other fixative devices anchoring the bone. The aim of this study is to explore the benefits of vibrational drilling (VD) in overcoming the complications associated with conventional drilling (CD). Drilling tests were performed on fresh cortical bone with the intention of investigating the effect of a range of frequencies, in combination with drilling speed and feed rate, on biological damage around the drilling region using histological sections of skeletally mature bone. The study examined the most influential factors and optimal combination of parameters for safe and efficient drilling in bone. Results from Taguchi grey relational analysis showed that a lower drilling speed and feed rate combined with a frequency of 20 kHz were favourable parameters for safe drilling in bone. Accordingly, VD using controlled parameters may be an alternative to CD in bone surgical procedures.

1. Introduction

Drilling of bone for repair, fixation, and reconstruction is a common surgical procedure in orthopaedics, traumatology, and dentistry. However, excessive drilling force and torque may lead to overstressing of bone and drill breakage, and may promote crack formation in bone structures [1–3]. The generation of heat above a threshold level during the process seriously affects cell activity, leading to necrotic bone (death of the cells) [4–6], and has been reported as a major cause of failure of fixative devices surrounded by bone [7]. The lower thermal transport capability of bone material is the principal factor that exposes bone tissue to heat [8]. Detailed information about the thermal osteonecrosis in bone was presented in a recently published review article [4]. The parameters that influence drilling effort and bone temperature are drill design, drilling speed, feed rate, bone type, drill bit quality (sharp or blunt), depth of drilling, and the use of coolant during the drilling process [4,9–12]. The mechanism by which external loadings produce changes in the physiological state of the bone is not well understood in the published literature. The destruction of osteocytes, which are the basic components of mature bone tissue, has been reported as the most detrimental outcome of the drilling process.

An osteocyte is a star-shaped cell that lies within a small irregular chamber (called a lacuna), and is considered to be mechanosensitive. External mechanical factors such as shear stress, hydrostatic pressure, and structural deformation induce complex physiological alterations in osteocytes [13–15]. Furthermore, osteocytes, as the mechano-sensing cells of the bone matrix, are sensitive to mechanical strain around them. It has been shown that straining the bone at slow and high rates influences the both the osteogenic response of the bone and bone formation [16–18]. More empty lacunae were observed from using microfracture than from drilling, which was attributed to the shearing and crushing of the adjacent bone under cooled irrigation [19]. The number of osteocytes found missing in the bone in drill-inserted sections was higher than in hammer-inserted sections [20]. A recent study investigated the effect of applied thrust force and blade speed on generating heat in bone [21], whereby the significance of factors affecting necrotic depth (as evidenced by empty lacunae) was determined. Though temperature was reported to be the most influential indicator for inducing thermal necrosis in bone, drilling force and torque were also prime contributors affecting the outcome of the process.

* Corresponding author.
E-mail address: kalam@squ.edu.om (K. Alam).

https://doi.org/10.1016/j.medengphy.2019.03.013
1350-4533/

The structural and functional connection between living bone tissue and fixative devices (such as screws and plates) is a complex topic. The bond between the bone and fixative device, and bone repair in the longer term, strongly depend on the extent of cell damage around the drilled site. The majority of studies have revealed that elevated temperatures arising from the cutting process are the major cause of bone necrosis. Drilling was observed to cause a lower level of osteocyte necrosis compared with microfracture [19]. Further, a noticeable ischaemia adjacent to the cut surface in the bone tissue has also been reported [22]. This phenomenon was attributed to thermal changes in response to drilling, which lead to protein coagulation and regional vasoconstriction.

Recent research has focused on exploring new techniques to minimise the invasiveness of the drilling process in bone. Vibrational drilling (VD) has recently been tested as an alternative to conventional drilling (CD) because VD can significantly reduce penetration force and torque, and induces lower temperature in bone when vibrational frequency control is imposed on the drill bit in the cutting direction [23–26]. However, despite the greater benefits VD can offer compared with CD, the biological response of bone to a range of vibrational frequencies has not yet been investigated. The histomorphometric characteristics of the healing stages in the tibia of a rat were studied using a single frequency of vibration for drilling [27]. Similar bone healing was found between piezosurgery and traditional bone drilling. Moreover, a recent study has shown less damage to bone cells when VD with a fixed frequency of 20 kHz and an amplitude of 16 µm was used in bovine cortical bone [28].

Because imposing micro-vibrations on the drill has been proposed as an enhancement mechanism in the design and development of automated surgical systems in orthopaedics and related fields, it is important to quantify the extent of cell damage in response to different parameters of vibration, particularly to frequency. As described previously, both elevated temperature and mechanical stress arising from bone drilling can affect the proliferation of living cell in the bone. Therefore, the outcome of the drilling process (temperature, force, and torque) in combination with a wide range of vibration frequencies is studied to investigate the quantitative damage to cells around the drilling region. This study aims to explore the benefits of VD in bone by investigating the biological response of bone using a series of drilling experiments and a comprehensive statistical analysis.

2. Materials and methods

2.1. Specimen for drilling

Drilling tests were performed on fresh bones excised from the middle diaphysis of a bovine femur. Cylindrical pieces of approximately 50 mm length were cut from the long femur bones. A total of eight healthy specimens of cylindrical shape were obtained from the femoral shafts, and each could accommodate between fifteen and twenty holes. Specimens were kept refrigerated at −10 °C to maintain their physical properties until being used in the experiments. Specimens were then transferred to a refrigerator, where the temperature was maintained at 20 °C, for 1 h before the drilling experiments. Specimens with sufficient moisture were then transferred to the drilling machine. A drill of 1 mm diameter was used to produce holes with a depth of up to approximately half the thickness of the cortical wall (4–5 mm from the top surface) in which to place the thermocouple for the specimen. Thermocouples (Type K) were inserted into the holes for the temperature measurements. The thermocouples were placed at a distance of 1 mm away from the drill track to avoid having the bead crushed by the cutting action of the drill bit. The holes drilled for the thermocouples were filled with thermal paste to eliminate the air gap between the bead of the thermocouple and the bone.

Table 1
Levels of parameters in bone drilling experiments.

Parameters (units)	Level 1	Level 2	Level 3	Level 4	Level 5
Drill speed (rpm)	1000	1500	2000	2500	3000
Feed (mm/min)	30	40	50	60	70
Frequency (kHz)	10	15	20	25	30

2.2. Drilling equipment and procedure

Drilling tests were performed on a vertical CNC machine. A transducer capable of producing vibrations up to 40 kHz and an amplitude of 30 µm in the drill was used in the drilling experiments. The experimental set-up for bone drilling, and the placement of the thermocouple in the bone specimen are shown in Fig. 1. Drilling tests were performed using 4.8 mm standard orthopaedic surgical drills (Orthofix, Italy) donated by the orthopaedic surgical department of a local hospital. The drilling region was continuously irrigated with sterile solution to mimic in-vivo drilling conditions, and all drilling tests were conducted at a room temperature of 28 °C. The drilling force and torque were measured using a two-component dynamometer (Type 9271A, Kistler).

2.3. Specimen for histological examination

The drilled specimens were fixed in 10% formaldehyde solution for 16 h immediately after the drilling procedure. Specimens were then decalcified in a solution of 40 ml 65 vol% nitric acid, 20 ml 10 vol% formaldehyde, and 340 ml distilled water for 48 h. A system microscope (BX53, Olympus) was used to visualise the viable osteocytes in the microstructure of the specimens. A digital microscope camera (DP22, Olympus) allowed observing, taking measurements, and acquiring images for analysis. Sections of bone for histological examination were taken from the same location where the thermocouple was placed. A schematic of the hole surface, and various depths at which cell damage was calculated are shown in Fig. 2. The percent cell damage, which represents the number of disappeared osteocytes from lacunae to the total number of osteocytes in the region specified for examination, was calculated. The numbers of filled and empty lacunae were measured in each half of the hole, and the percent damage was calculated. Cell viability was measured at a depth of 600 µm because this depth it is critical for the osseointegration of surrounding fixative devices.

2.4. Drilling parameters

Frequency of vibration, drill speed, and feed rate were selected as parameters for statistical analysis. Five levels of each of the drilling parameters provided in Table 1 were considered in the experiments. The effect of drilling parameters was analysed in terms of four different responses: force, torque, temperature, and cell loss. The objective of the statistical analysis was to identify a combination of drilling parameters for the minimum values of response variables for safe drilling in bone.

2.5. Design of experiment

Specially designed orthogonal arrays (based on the Taguchi method), which used optimal settings of process parameters with a minimum number of experiments, were used to collect data for the response variables [29]. The Taguchi technique was combined with grey relational analysis (GRA) to optimise the multi-process

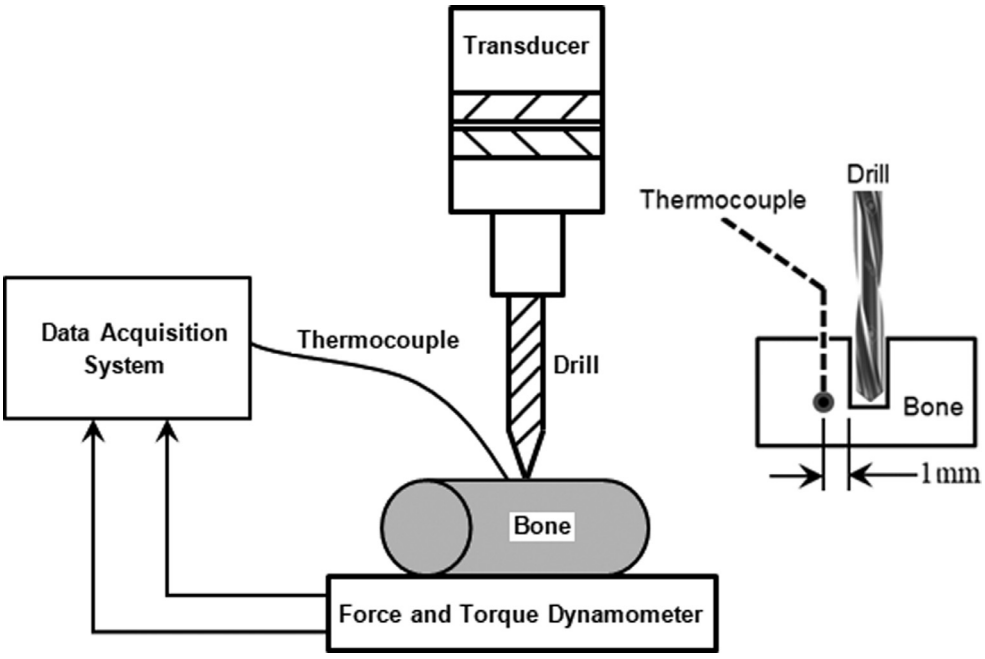

Fig. 1. Schematic of bone drilling system and data acquisition system.

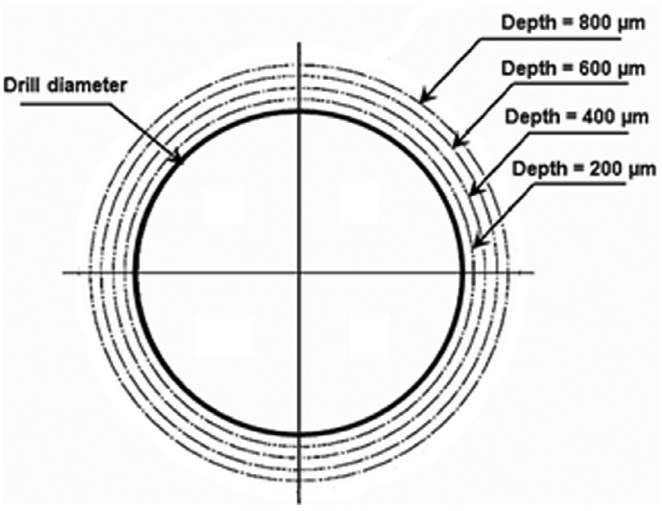

Fig. 2. Schematic of the drilled hole and measurements of cell damage at various depths.

parameters for multiple response variables. The Taguchi GRA uses the signal-to-noise (S/N) ratio, which is the ratio of the mean to the standard deviation, to calculate the grey relational grade (GRG) of response variables [30]. The following steps were used to calculate the GRG.

2.5.1. S/N ratio for response variables

Taguchi classifies the response function into three types: larger-the-better, smaller-the-better, and nominal-the-better [31]. All response variables considered in this research were to be minimised. Therefore, the smaller-the-better type of S/N ratio was used and calculated with the following equation:

$$x_i^o(k) = -10\log_{10}\left(\frac{1}{n}\sum_{i=1}^{n} y_i^2(k)\right) \tag{1}$$

In the above equation, $x_i^o(k)$ represents the S/N ratio for response i observed at the kth trial, n is the total number of experimental trials, and $y_i\ (k)$ is the observed value.

2.5.2. Normalisation of the value

It is recommended to normalise the S/N ratio rather than the observed response variable in GRA [32]. The use of formulae for normalising the S/N ratio also depends on whether the response needs to be maximised or minimised. As all responses needed to be minimised, Eq. (2) was utilised for normalisation.

$$z_i^*(k) = \frac{x_i^o(k) - min\ x_i^o(k)}{max\ x_i^o(k) - min\ x_i^o(k)} \tag{2}$$

In Eq. (2), $max\ x_i^o(k)$ and $min\ x_i^o(k)$ represent the largest and smallest S/N values for response i across all the experiments.

2.5.3. Calculating grey relational coefficient (GRC)

The GRC helps to express the correlation between normalised data with the ideal result.

$$\gamma_i(k) = \frac{\Delta_{min} + \zeta\,\Delta_{max}}{\Delta_i(k) + \zeta\,\Delta_{max}} \tag{3}$$

In Eq. (3), ζ is a distinguishing coefficient, the value of which varies within the range (0, 1). $\Delta_i(k)$ in the equation is the distance between the normalised value and reference sequence for the ith response at the kth trial. $\Delta_{\max}$ and $\Delta_{\min}$ are the maximum and minimum values of $\Delta_i(k)$, respectively.

$$\Delta_i(k) = |z_o^*(i) - z_i^*(k)| \tag{4}$$

$z_o^*(i)$ in Eq. (4) is the maximum value of $z_i^*(k)$, and it represents a reference sequence.

2.5.4. Calculating the GRG

The GRG is a unified weighted average value of the GRC of all the response variables. If equal weight is given to all response variables, then the GRG can be calculated using the following equation:

$$\delta = \frac{1}{n}\sum_{i=1}^{n} \mathrm{Y}_i(k) \tag{5}$$

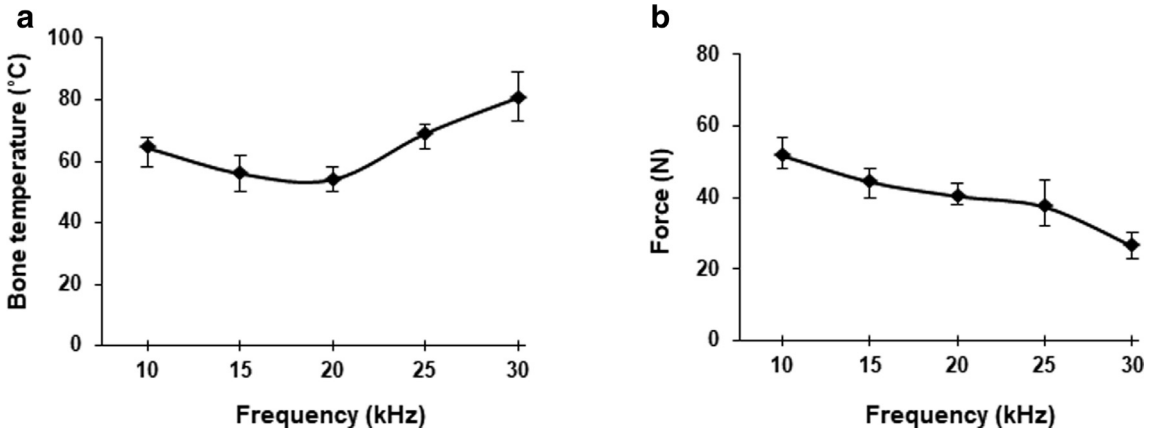

Fig. 3. (a) Variation in bone temperature with frequency of vibration, (b) variation in drilling thrust force with frequency of vibration (drill speed – 2000 rpm; feed rate – 50 mm/min).

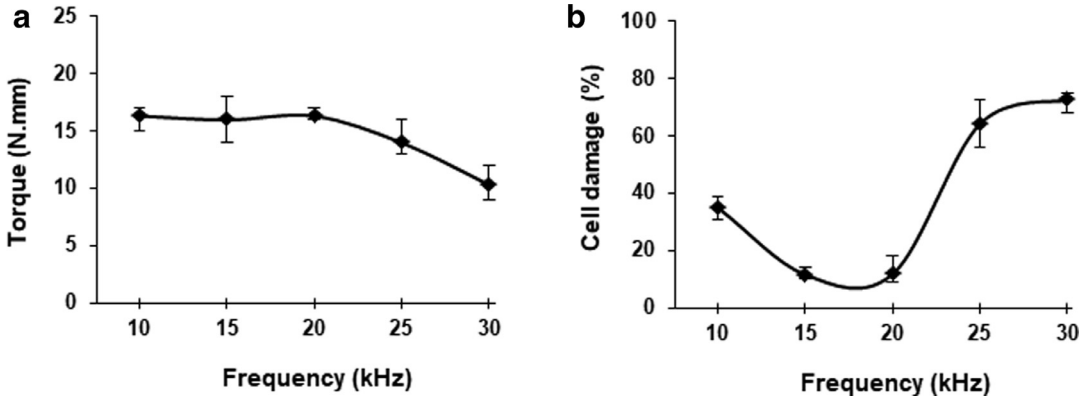

Fig. 4. (a) Variation in torque with frequency of vibration, (b) cell damage with frequency of vibration (measurement depth – 600 µm).

3. Results

The number of disappeared osteocytes surrounding the drilled cut surface was calculated and correlated with drill speed, feed rate, and frequency of vibration. All reported values of force, torque, and temperature are their peak stabilised values. A detailed statistical analysis is performed in the subsequent section to evaluate the effect of frequency on bone temperature, force, and torque in combination with various drilling speeds and feed rates. A few representative plots are discussed here. Each data point in the following plots (Figs. 3–5) represents the average of three consecutive tests using the same drilling parameters. The small bar attached to each data point represents the upper and lower bounds of the experimentally measured values. The variation in bone temperature, force, and torque against frequency is shown in Fig. 3 and 4(a) for a drilling speed of 2000 rpm and a feed rate of 50 mm/min. The bone temperature decreased slightly when the frequency was increased from 10 to 20 kHz; Fig. 3(a). A significant increase in bone temperature was noted when the frequency was further increased to 30 kHz. There was a significant reduction in force and torque with an increase in the frequency of vibration; Fig. 3(b) and 4(a). The calculated percent cell damage in the radial direction for a range of vibrational frequencies at a depth of 600 µm is shown in Fig. 4(b). Fig. 5 shows the amount of cell damage at various depths measured from the cut surface for a frequency of vibration of 30 kHz, drill speed of 2000 rpm, and feed rate of 50 mm/min. The disappearance of cells from lacunae (cell damage) was found to decrease, and then severely increase for the frequency range

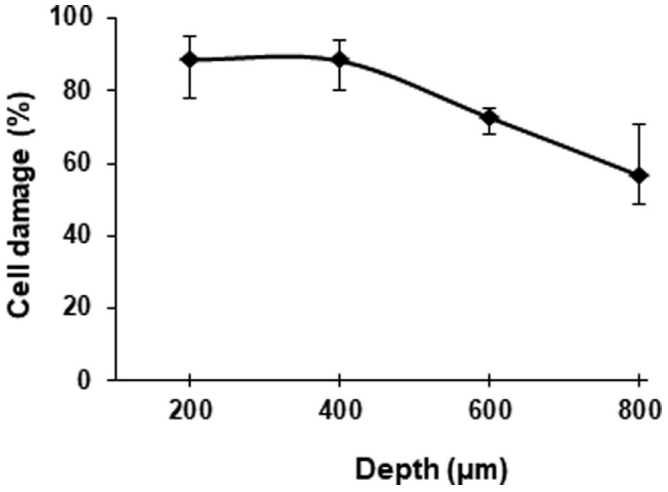

Fig. 5. Cell loss at different levels of depth from the cut surface (frequency – 30 kHz; drill speed – 2000 rpm; feed rate – 50 mm/min).

used in the experiments. As expected, the cell damage was found to significantly decrease with distance away from the cut surface.

Histological images showing viable osteocytes within the lacunae (dark spots indicated by the arrows) are shown in Fig. 6 and 7. The locations of viable osteocytes within the lacunae are shown with arrows, and empty lacunae are shown with circles. Haversian canals, which are series of microscopic tubes providing pas-

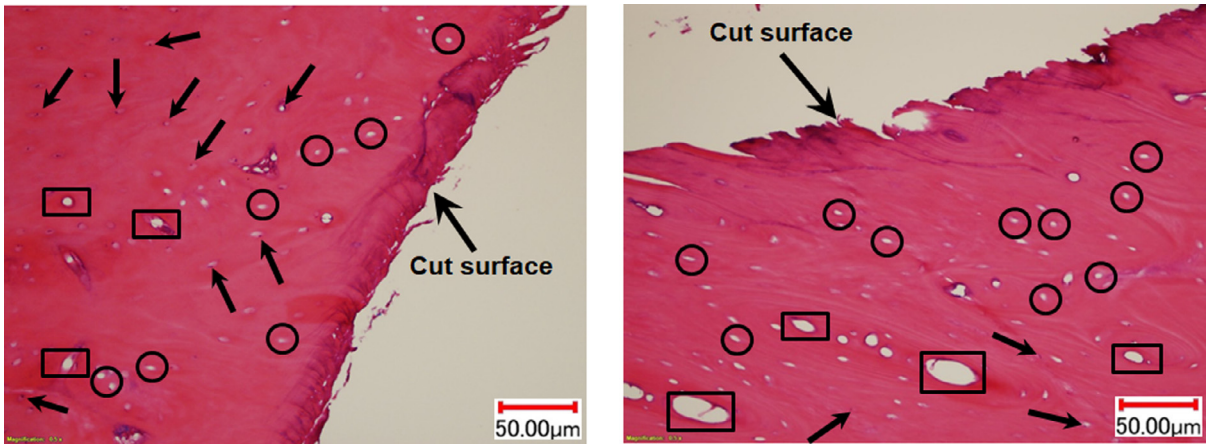

Fig. 6. Histopathology of the drilled specimens in CD. Left – low drilling speed (1000 rpm), right – high speed drilling (3000 rpm).

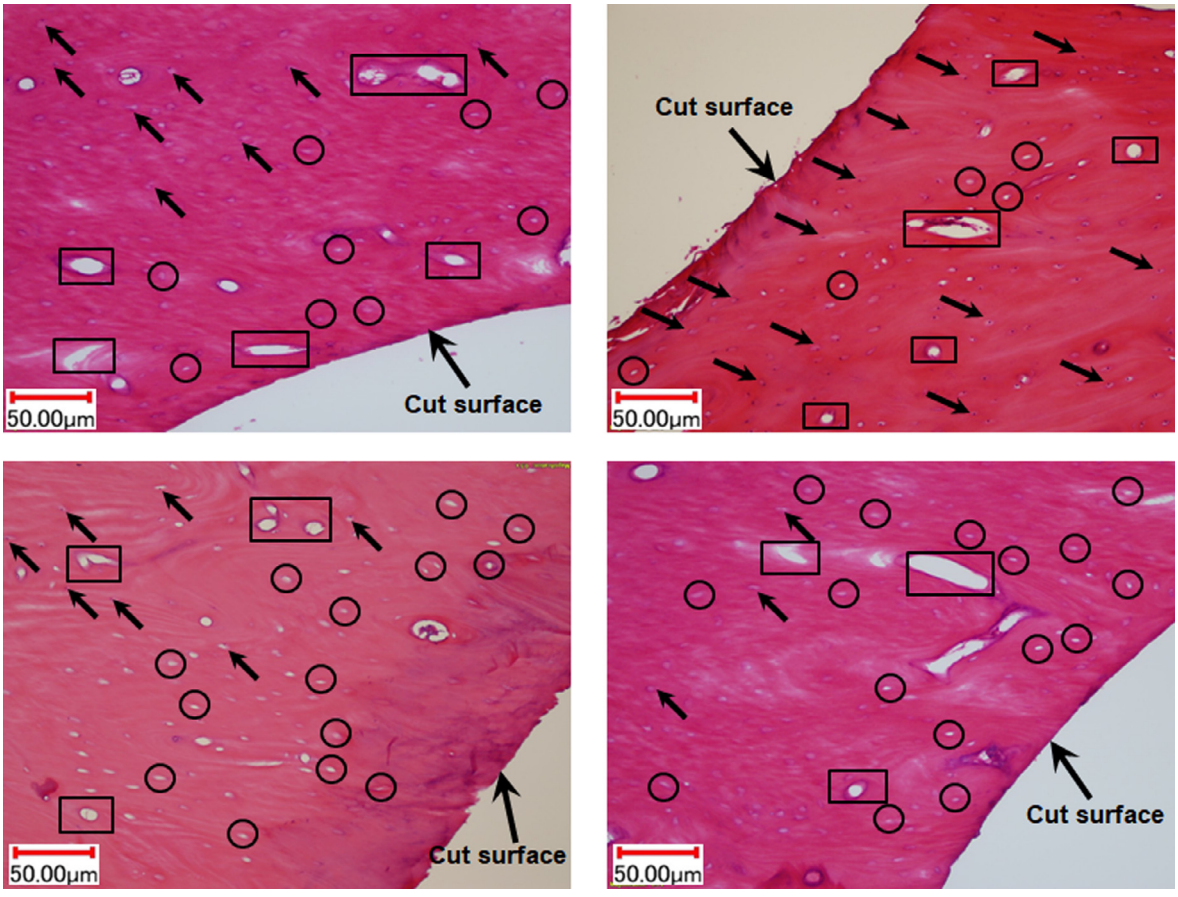

Fig. 7. Histopathology of drilled specimens in VD. Top row, left: frequency – 10 kHz; right: frequency – 20 kHz; bottom row, left: frequency – 25 kHz; right: frequency – 30 kHz.

sage to the blood vessels and nerves, are enclosed with rectangles. The absence of osteocytes in the osteocyte lacunae (encircled) indicates that the cells are dead and have been resorbed in the bone. Only a few osteocytes, lacunae, and Haversian canals are highlighted in Fig. 6 and 7 to avoid populating the images with labels and allow readers to see most of the biological and structural entities. The histopathology of specimens drilled by CD and VD using a fixed drill speed and feed rate are shown in Fig. 6 and 7. Damaged cells after CD using minimum and maximum speeds at a feed rate of 50 mm/min are shown in Fig. 6. More cells were found to be missing when a higher drill speed was used in CD. A comparison of the damaged cells resulting from different frequency values is shown in Fig. 7. Because the measured temperature was almost the same while frequencies of 15 and 20 kHz were used, a histology plot for only 20 kHz is provided in Fig. 7. Less cell damage was found when frequencies of 15 and 20 kHz were used. Frequencies above 20 kHz significantly increased the damage around the cut surface (Fig. 7).

Because the variation trends for bone temperature, force, and torque using a range of drilling speeds, feed rates, and frequencies of vibration are quite dissimilar, statistical analysis was performed to identify favourable drilling parameters in the next section.

Table 2
Taguchi experimental set-up and observed response variables. All values of cell loss were measured at 600 µm depth.

Exp.	Experimental set up			Response variable							
	Speed (rpm)	Feed rate (mm/min)	Frequency (kHz)	Force (N)		Torque (N mm)		Temp (C)		Cell lost (%)	
				Avg.	Std. dev	Avg.	Std. dev	Avg.	Std. dev	Avg.	Std. dev
1	1000	30	10	53	2.00	17	2.00	47	3.46	12	1.00
2	1000	40	15	51	3.00	17	1.00	47	2.65	8	1.73
3	1000	50	20	47	3.00	17	0.00	51	1.00	5	0.00
4	1000	60	25	65	2.65	18	1.73	66	3.61	69	5.20
5	1000	70	30	38	2.00	11	0.00	71	3.00	81	3.61
6	1500	30	15	45	3.00	14	2.65	51	1.73	15	1.00
7	1500	40	20	45	1.00	12	1.73	53	1.73	11	1.73
8	1500	50	25	35	2.65	14	1.73	68	2.65	55	3.46
9	1500	60	30	48	2.00	15	2.00	66	2.65	49	1.73
10	1500	70	10	61	4.58	15	3.00	68	2.65	28	3.46
11	2000	30	20	40	2.00	13	1.00	48	3.61	10	2.65
12	2000	40	25	36	2.00	12	1.73	71	4.58	55	4.36
13	2000	50	30	26	1.00	10	2.00	80	4.36	73	5.29
14	2000	60	10	53	2.65	16	3.46	69	2.65	45	3.61
15	2000	70	15	50	2.65	13	0.00	62	4.36	22	1.00
16	2500	30	25	28	1.00	9	1.00	66	1.73	52	3.61
17	2500	40	30	22	1.00	11	2.65	73	3.00	55	3.46
18	2500	50	10	45	3.46	15	1.00	65	3.46	55	2.00
19	2500	60	15	47	1.73	16	1.73	61	1.00	18	0.00
20	2500	70	20	51	1.73	9	2.65	62	3.61	25	2.00
21	3000	30	30	21	1.73	8	2.00	77	4.58	61	3.61
22	3000	40	10	43	2.65	11	2.65	71	3.61	45	2.65
23	3000	50	15	40	3.46	12	1.73	65	2.00	16	0.00
24	3000	60	20	44	1.73	14	1.00	65	1.73	24	1.73
25	3000	70	25	50	2.65	11	1.73	80	3.46	90	4.58

4. Statistical analysis

The experimental set-up using a Taguchi orthogonal array (L25 orthogonal array) and associated response variables were as shown in Table 2. Again, each data point is the average of three consecutive drilling tests. Standard deviation, which indicates dispersion of data about the average value, is also shown. Based on the Taguchi GRA method as discussed in Section 2.5, the observed response variables (Table 2) were translated to an S/N ratio after their normalised values were calculated. Higher values of normalised S/N ratio indicate better performance, and the reverse is also true. Individual best performance characteristics are represented by the normalised value of one, and worst performance by zero. Table 3 shows the S/N ratio and normalised values of all response variables.

The GRC was computed based on the normalised value of the S/N ratio. While computing GRC, equal importance was given to the maximum and minimum absolute deviation [33]. The GRG was then calculated by taking the average GRC of all response variables. Table 4 shows the GRC, GRG, and ranking of all experimental set-ups. It can be seen that experimental set-up 21 represents the optimised combination (highest GRG value): a speed of 3000 rpm, feed rate of 30 mm/min, and frequency of 30 kHz. This set-up is represented by A5-B1-C5. Moreover, the lowest GRG is obtained for the set-up A1-B4-C4 in Table 5.

4.1. Significant process parameters

To estimate the effect of each process parameter on the responses, the average GRA of each parameter was used along with all levels of other process parameters. The average response value at different levels of the control parameters are shown in Table 5 and Fig. 8. It can be seen that a drill speed of 1000 rpm, feed rate of 30 mm/min, and frequency of 20 kHz (experimental set-up A1-B1-C3) are the optimum values for safe drilling in bone. The parameter with the maximum difference in average GRG values in Table 5 indicates the parameter with the highest influence. This means that feed rate is the most dominant parameter in VD, followed by frequency and drill speed.

4.2. Confirmation test

A confirmatory experiment was suggested to validate the accuracy of the optimised parameters and to determine the improvement in performance characteristics. It was necessary to first predict GRG based on the optimised processes parameters obtained from Table 5.

$$\delta_{pre} = \delta_{tot} + \sum_{i=1}^{n} (\delta_{opt} - \delta_{tot}) \tag{6}$$

Here, δ_{tot} represents the total mean of GRG, δ_{opt} is the mean of GRG at the optimal level of each process parameter, and n is the number of parameters. Based on Eq. (6), the predicted GRG is obtained as 0.699. Table 6 shows the results of a confirmation test using the optimal process parameters estimated using the GRA method. It can be seen that the GRG for the confirmation test is 0.722, which shows an improvement of 6.33% from the initial optimal setting. To conclude, the process parameters estimated through the GRA method offer the optimal performance characteristics of all the combinations of various levels of process parameters.

5. Discussion

Surgical drills used for drilling holes in bone do not have a mechanism for measuring the drilling force, torque, and temperature during the incision. In the current study, the prescribed measurements were obtained using a CNC drilling machine equipped with sensors for force, torque, temperature, and a transducer for generating a range of frequencies. The obtained results mimic a situation where a hand surgical drill would be used, because the mechanics of cutting remain the same. Lower drilling speed and frequency, and higher feed rates, produced higher drilling force. A recent study found a significant increase in drilling force when a

Table 3
S/N ratio and normalised values of responses.

Exp.	S/N ratio				Normalised value of S/N ratio			
	Force	Torque	Temp.	Cell lost	Force	Torque	Temp.	Cell lost
1	−34.486	−24.609	−33.442	−21.584	0.181	0.070	1.000	0.697
2	−34.151	−24.609	−33.442	−18.062	0.215	0.070	1.000	0.837
3	−33.442	−24.609	−34.151	−13.979	0.287	0.070	0.846	1.000
4	−36.258	−25.105	−36.391	−36.777	0.000	0.000	0.362	0.092
5	−31.596	−20.828	−37.025	−38.170	0.475	0.607	0.224	0.036
6	−33.064	−22.923	−34.151	−23.522	0.325	0.310	0.846	0.620
7	−33.064	−21.584	−34.486	−20.828	0.325	0.500	0.774	0.727
8	−30.881	−22.923	−36.650	−34.807	0.548	0.310	0.306	0.170
9	−33.625	−23.522	−36.391	−33.804	0.268	0.225	0.362	0.210
10	−35.707	−23.522	−36.650	−28.943	0.056	0.225	0.306	0.404
11	−32.041	−22.279	−33.625	−20.000	0.430	0.401	0.960	0.760
12	−31.126	−21.584	−37.025	−34.807	0.523	0.500	0.224	0.170
13	−28.299	−20.000	−38.062	−37.266	0.811	0.725	0.000	0.072
14	−34.486	−24.082	−36.777	−33.064	0.181	0.145	0.278	0.240
15	−33.979	−22.279	−35.848	−26.848	0.232	0.401	0.479	0.487
16	−28.943	−19.085	−36.391	−34.320	0.745	0.855	0.362	0.190
17	−26.848	−20.828	−37.266	−34.807	0.959	0.607	0.172	0.170
18	−33.064	−23.522	−36.258	−34.807	0.325	0.225	0.390	0.170
19	−33.442	−24.082	−35.707	−25.105	0.287	0.145	0.510	0.557
20	−34.151	−19.085	−35.848	−27.959	0.215	0.855	0.479	0.443
21	−26.444	−18.062	−37.730	−35.707	1.000	1.000	0.072	0.135
22	−32.669	−20.828	−37.025	−33.064	0.366	0.607	0.224	0.240
23	−32.041	−21.584	−36.258	−24.082	0.430	0.500	0.390	0.598
24	−32.869	−22.923	−36.258	−27.604	0.345	0.310	0.390	0.457
25	−33.979	−20.828	−38.062	−39.085	0.232	0.607	0.000	0.000

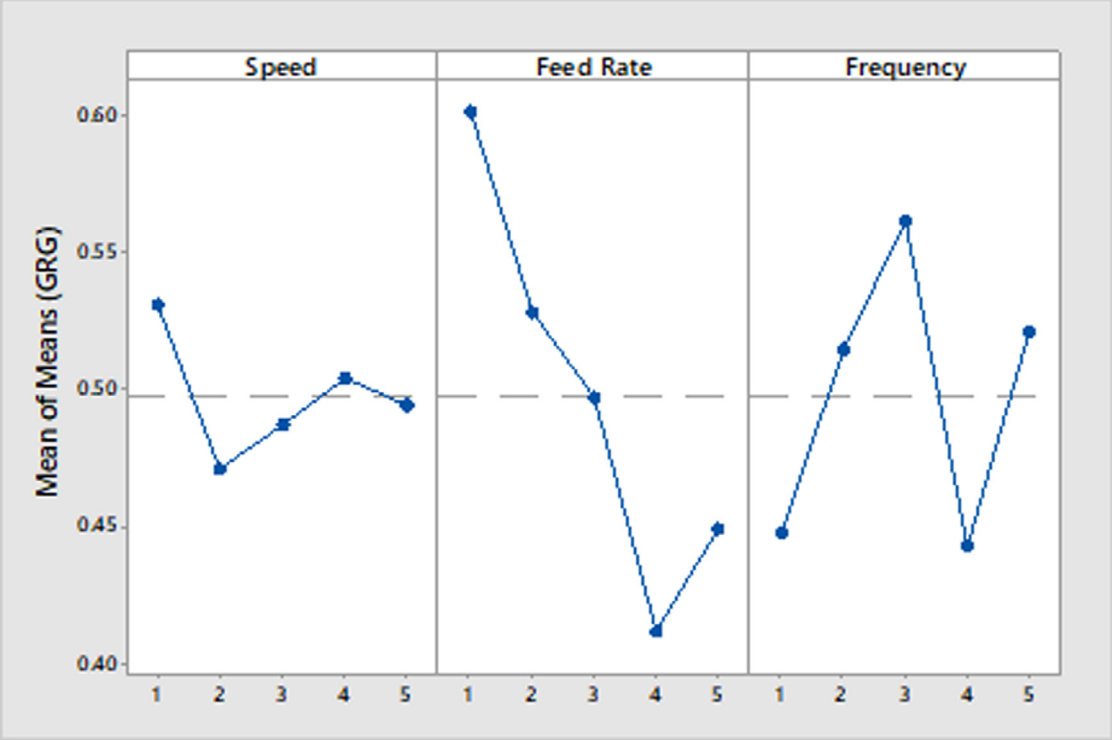

Fig. 8. Effect of process parameters on GRG at different levels.

drilling speed of less than 1000 rpm was used [23]. The increase in the drilling force was attributed to slow and inefficient evacuation of chips from the drilling region. The engagement and disengagement of the drill cutting lips with the bone (as a result of vibration) affects the ability of the cutting lips of the drill to generate moment about the longitudinal axis of the drill bit. Using a frequency above 20 kHz caused additional heat generation from the mechanical vibrations of the drill, which dissipated into the bone tissue. However, using a frequency within the range of 15–20 kHz had the benefit of reducing friction because the alternating contact of the drill with the bone, which produced lower heat, was dominant over the heat dissipation caused by the mechanical vibrations of the drill. Moreover, a lower feed rate could minimise the disappearance of osteocytes because it would generate less heat due to the reduction in friction. The cell damage near the immediate vicinity of the cutting region was greater due to elevated stress and

Table 4
Grey relational coefficient (GRC), grey relational grade (GRG), and ranking of experimental set-ups.

Exp.	Grey relational coefficient (GRC)				GRG	Rank
	Force	Torque	Temp.	Cell lost		
1	0.379	0.350	1.000	0.623	0.588	5
2	0.389	0.350	1.000	0.755	0.623	4
3	0.412	0.350	0.765	1.000	0.632	2
4	**0.333**	**0.333**	**0.439**	**0.355**	**0.365**	**25**
5	0.488	0.560	0.392	0.342	0.445	17, 18
6	0.426	0.420	0.765	0.568	0.545	9
7	0.426	0.500	0.689	0.647	0.565	6, 7
8	0.525	0.420	0.419	0.376	0.435	19
9	0.406	0.392	0.439	0.388	0.406	21
10	0.346	0.392	0.419	0.456	0.403	23
11	0.467	0.455	0.927	0.676	0.631	3
12	0.512	0.500	0.392	0.376	0.445	17, 18
13	0.726	0.645	0.333	0.350	0.514	11
14	0.379	0.369	0.409	0.397	0.389	24
15	0.394	0.455	0.490	0.494	0.458	13
16	0.663	0.775	0.439	0.382	0.565	6, 7
17	0.924	0.560	0.377	0.376	0.559	8
18	0.426	0.392	0.451	0.376	0.411	20
19	0.412	0.369	0.505	0.530	0.454	14
20	0.389	0.775	0.490	0.473	0.532	10
21	**1.000**	**1.000**	**0.350**	**0.366**	**0.679**	**1**
22	0.441	0.560	0.392	0.397	0.447	15
23	0.467	0.500	0.451	0.554	0.493	12
24	0.433	0.420	0.451	0.480	0.446	16
25	0.394	0.560	0.333	0.333	0.405	22

temperature. Lower drilling force and torque may help to prevent overstressing the bone, avoid drill breakage, preserve the structure, and decrease intra- and post-operative bleeding.

Previous studies have described bone formation, remodelling, and osseointegration as indictors for successful and efficient osteotomies using piezo surgery, CD, and sawing of bone. The exact temperature level for inducing necrosis in bone was reported to be within the range of 50–70 °C [4,9,34]. A histological examination of drilled specimens provided a means of determining the effect of drilling parameters on bone health. Fewer necrotic cells from drilling bovine cortical bone, as evidenced by the depth of empty lacunae, were found when the drilling force was increased [35]. Irrigating the cutting region with saline has been shown to produce lower heat, less thermal damage, and increased osteocyte viability during the sawing and burring of cortical bone [36]. A large drilling force was reported to generate miniature cracks within the microstructure of the bone tissue [25,26], and it was expected that the cells were buried in the newly generated cavities. An inverse relationship between drilling force and bone temperature reported in the literature [6,37] has complicated the identification of favourable drilling parameters in surgical bone incision.

Research related to bone cutting has mainly been performed using conventional cutting tools such as a drill, bur, saw blades, and tools with superimposed micro-vibrations (piezosurgery). Vibrational cutting has demonstrated greater viability of cells and enhanced bone healing compared with conventional cutting. Piezotomes have presented a new gold standard in bone cutting due to improved healing, less bone loss, precision, soft tissue protection, and reduced intra-surgical and post-surgical morbidity [38].

Table 6
Confirmation test.

	Initial setting	Prediction	Experimental
Setting level	A5-B1-C5	Al-B1-C3	Al-B1-C3
Force	21	–	38
Torque	8	–	10
Temperature	77	–	47
Cell Loss	61	–	8
Grey relational grade	0.679	0.699	0.722
Percentage improvement in the GRG			6.33%

Bone particulate collected by a piezoelectric system at a frequency of 35 kHz has greater potential for longevity than that collected by a conventional rotary system [39]. Better cell viability in piezosurgery has been attributed to vibrational movements and reduced pressure from the surgical tool, resulting in insignificant thermal alteration in the bone tissue. While performing osteotomy using a bone scalpel with a 0.5 mm width, 3 mm length, and five cutting teeth, piezoelectric surgery resulted in faster bone formation and remodelling in the nasal bones of rabbits [40]. Autogenous bone grafts harvested with a manual instrument and piezosurgery had more viable cells in comparison with bone chips harvested with a conventional rotary device [41]. Bone specimens were harvested using a mini periodontal chisel, a low-speed handpiece, and piezosurgery. The viability of osteoblast cells was 48.80 ± 4.05% for the manual instrument group, 39.64 ± 5.40% for the rotary device group, and 49.92 ± 5.09% for the piezosurgery group. The values of the regenerated bone area with respect to the total osteotomy area were approximately double for piezoelectrical devices compared with conventional rotary osteotomes [42]. In contrast to the above studies, bone healing after piezosurgery in rat tibial bone was found to be similar to that observed with CD [27]. None of the aforementioned studies provided quantitative analysis of bone viability with regard to the range of frequency and extent of cell damage in the bone surrounding the cut surface.

6. Limitations

Structural composition such as the volume fraction of organic and inorganic constituents of the bone, orientation of osteons, volume fraction of lacunae and Haversian canals, and number of cells at various layers was slightly different. However, due to the extremely complex microstructure of bone, it is not possible to look into this issue in the current study. We assumed that the properties, microstructure, and constituents of bone were the same at all levels along the wall thickness of the cortical bone. This study did not explore the effect of alternating stress reversals, arising from high frequency micro-vibrations, on the physiological structure of the bone. The temperature captured in the region up to 1 mm distance from the drilling track was assumed to be the same as that of the cut surface due to the compact nature of the bone. However, this assumption may not be true in the case if trabecular (spongy) bone, where the effect of porosity cannot be ignored. A depth of 600 µm considered in the current study was the expected crucial depth for determining the strength of fixation between the bone and the anchoring metallic device. Further research is

Table 5
Response table for grey relational grade.

Control parameter	Level 1	Level 2	Level 3	Level 4	Level 5	Max–min	Rank
Speed (A)	**0.531**	0.471	0.487	0.504	0.494	0.060	3
Feed (B)	**0.601**	0.528	0.497	0.412	0.449	0.190	1
Frequency (C)	0.448	0.515	**0.609**	0.443	0.521	0.166	2

required to find the relationship between the extent of damage, and osseointegration and bone formation surrounding implants or fixative elements.

7. Conclusion

Large drilling forces and higher bone temperatures (resulting from the drilling process) are detrimental to the delicate structure of bone. This study hypothesised that controlled drilling parameters in combination with a frequency of 20 kHz would be a favourable combination for safe drilling in bone. Analysis showed that the process of bone drilling was mainly affected by feed rate, followed by frequency and drill speed. The drilling force, torque, temperature, and cell loss could be minimised when the drill speed was maintained at 1000 rpm, the feed rate at 30 mm/min, and the frequency at 20 kHz. Frequencies above 20 kHz significantly reduced drilling force and torque, but increased bone temperature significantly above the thermal threshold level sufficient for inducing necrosis in bone.

Evaluating the effect of high levels of stress reversal in vibrational drilling on the physiology of bone cells is beyond the scope of this study. The existing hand-held bone surgical drill can be modified to operate at a single frequency of vibration for safe drilling in bone. A prototype of a hand-held drilling system is to be designed to facilitate real-time measurement of force, torque, and temperature during surgical incision.

Conflicts of interest

None.

Funding

This research study is partially supported by Internal Grant Scheme of Sultan Qaboos University, Sultanate of Oman (Grant No: IG/ENG/MIED/16/02).

Acknowledgment

The authors are thankful to Mr. Bader Al-Sumri, technician, Department of Pathology, Sultan Qaboos University for the preparation of specimens for histological examination. The authors would also like to thank Dr. Asim Qureshi, consultant, Department of Pathology, Sultan Qaboos University for his support.

References

[1] Brett PN, Baker DA, Taylor R, Griffiths MV. Controlling the penetration of flexible bone tissue using the stapedotomy microdrill. Proc Inst Mech Eng Part I J Syst Control Eng 2004;218(5):343–51.
[2] Kasiri S, Reilly G, Taylor D. Wedge indentation fracture of cortical bone: experimental data and predictions. J Biomech Eng 2010;132(8):081009.
[3] Bassi JL, Pankaj M, Navdeep S. A technique for removal of broken cannulated drill bit: Bassi's method. J Ortho Trauma 2008;22(1):56–8.
[4] Augustin G, Zigman T, Davila S, Udilljak T, Staroveski T, Brezak D, Babic S. Cortical bone drilling and thermal osteonecrosis. Clin Biomech 2012;27(4):313–25.
[5] Eriksson AR, Albrektsson T, Albrektsson B. Heat caused by drilling cortical bone: temperature measured in vivo in patients and animals. Acta Orthop Scand 1984;55(6):629–31.
[6] Bachus KN, Rondina MT, Hutchinson DT. The effects of drilling force on cortical temperatures and their duration: an in vitro study. Med Eng Phys 2000;22(10):685–91.
[7] Athanasou NA. The pathobiology and pathology of aseptic implant failure. Bone Joint Res 2016;5(5):162–8.
[8] Davidson SR, James DF. Drilling in bone: modeling heat generation and temperature distribution. J Biomech Eng 2003;125(3):305–14.
[9] Pandey RK, Panda SS. Drilling of bone: a comprehensive review. J Clin Orthop Trauma 2013;4(1):15–30.
[10] Kalidindi V. Optimization of drill design and coolant systems during dental implant surgery. University of Kentucky; 2004.
[11] Alam K, Imran SH, Al-Shabibi A, Ghodsi M, Silberschmidth V. Experimental study on the effect of drill quality on bone temperature. Biomed Eng App Bas C 2018;30(02):1850018.
[12] Alam K, Ghodsi M, Al-Shabibi A, Silberschmidt V. Experimental study on the effect of point angle on force and temperature in vibrational bone drilling. J Med Biol Eng 2018;38(2):236–43.
[13] Jacobs CR, Temiyasathit S, Castillo AB. Osteocyte mechanobiology and pericellular mechanics. Annu Rev Biomed Eng 2010;12:369–400.
[14] Chen JH, Liu C, You L, Simmons CA. Boning up on Wolff's law: mechanical regulation of the cells that make and maintain bone. J Biomech 2010;43(1):108–118.
[15] Thompson WR, Rubin CT, Rubin J. Mechanical regulation of signaling pathways in bone. Gene 2012;503(2):179–93.
[16] Price C, Zhou X, Li W, Wang L. Real-time measurement of solute transport within the lacunar-canalicular system of mechanically loaded bone: direct evidence for load-induced fluid flow. J Bone Miner Res 2011;26(2):277–85.
[17] Robinson JA, Chatterjee-Kishore M, Yaworsky PJ, Cullen DM, Zhao W, Li C, Kharode Y, Sauter L, Babij P, Brown EL, Hill AA. Wnt/β-catenin signaling is a normal physiological response to mechanical loading in bone. J Biol Chem 2006;281(42):31720–8.
[18] Luo G, Cowin SC, Sadegh AM, Arramon YP. Implementation of strain rate as a bone remodeling stimulus. J Biomech Eng 1995;117(3):329–38.
[19] Chen H, Sun J, Hoemann CD, Lascau-Coman V, Ouyang W, McKee MD, Shive MS, Buschmann MD. Drilling and microfracture lead to different bone structure and necrosis during bone-marrow stimulation for cartilage repair. J Orthop Res 2009;27(11):1432–8.
[20] Franssen BB, Van Diest PJ, Schuurman AH, Kon M. Keeping osteocytes alive: a comparison of drilling and hammering K-wires into bone. J Hand Surg-Eur Vol 2008;33(3):363–8.
[21] James TP, Chang G, Micucci S, Sagar A, Smith EL, Cassidy C. Effect of applied force and blade speed on histopathology of bone during resection by sagittal saw. Med Eng Phys 2014;36(3):364–70.
[22] Field JR, Sumner-Smith G. Bone blood flow response to surgical trauma. Injury 2002;33(5):447–51.
[23] Alam K, Mitrofanov AV, Silberschmidt VV. Experimental investigations of forces and torque in conventional and ultrasonically-assisted drilling of cortical bone. Med Eng Phys 2011;33(2):234–9.
[24] Alam K, Silberschmidt VV. Analysis of temperature in conventional and ultrasonically-assisted drilling of cortical bone with infrared thermography. Technol Health Care 2014;22(2):243–52.
[25] Alam K, Ahmed N, Silberschmidt VV. Comparative study of conventional and ultrasonically-assisted bone drilling. Technol Health Care 2014;22(2):253–62.
[26] Wang Y, Cao M, Zhao Y, Zhou G, Liu W, Li D. Experimental investigations on microcracks in vibrational and conventional drilling of cortical bone. J Nanomater 2013;5:845205.
[27] Esteves JC, Marcantonio E Jr, de Souza Faloni AP, Rocha FR, Marcantonio RA, Wilk K, Intini G. Dynamics of bone healing after osteotomy with piezosurgery or conventional drilling–histomorphometrical, immunohistochemical, and molecular analysis. J Transl Med 2013;11(1):221–33.
[28] Singh G, Jain V, Gupta D, Sharma A. Parametric effect of vibrational drilling on osteonecrosis and comparative histopathology study with conventional drilling of cortical bone. Proc Inst Mech Eng H 2018;232(10):975–86.
[29] Ahmad N, Kamal S, Raza ZA, Hussain T, Anwar F. Multi-response optimization in the development of oleo-hydrophobic cotton fabric using Taguchi based grey relational analysis. Appl Surf Sci 2016;367:370–81.
[30] Pang JS, Ansari MN, Zaroog OS, Ali MH, Sapuan SM. Taguchi design optimization of machining parameters on the CNC end milling process of halloysite nanotube with aluminium reinforced epoxy matrix (HNT/Al/Ep) hybrid composite. HBRC J 2014;10(2):138–44.
[31] Nelabhotla DM, Jayaraman TV, Asghar K, Das D. The optimization of chemical mechanical planarization process-parameters of c-plane gallium-nitride using Taguchi method and grey relational analysis. Mater Des 2016;104:392–403.
[32] Haq AN, Marimuthu P, Jeyapaul R. Multi response optimization of machining parameters of drilling Al/SiC metal matrix composite using grey relational analysis in the Taguchi method. Int J Adv Manuf Tech 2008;37(3–4):250–5.
[33] Kuo Y, Yang T, Huang GW. The use of a grey-based Taguchi method for optimizing multi-response simulation problems. Eng Optimiz 2008;40(6):517–28.
[34] Berman AT, Reid JS, Yanicko DR Jr, Sih GC, Zimmerman MR. Thermally induced bone necrosis in rabbits. Relation to implant failure in humans. Clin Orthop Relat R 1984:284–92.
[35] Karaca F, Aksakal B, Kom M. Influence of orthopaedic drilling parameters on temperature and histopathology of bovine tibia: an in vitro study. Med Eng Phys 2011;33(10):1221–7.
[36] Tawy GF, Rowe PJ, Riches PE. Thermal damage done to bone by burring and sawing with and without irrigation in knee arthroplasty. J Arthroplasty 2016;31(5):1102–8.
[37] Matthews LS, Hirsch C. Temperatures measured in human cortical bone when drilling. J Bone Joint Surg Am 1972;54(2):297–308.
[38] Troedhan A, Mahmoud ZT, Wainwright M, Khamis MM. Cutting bone with drills, burs, lasers and piezotomes: a comprehensive systematic review and recommendations for the clinician. Int J Oral Craniofac Sci 2017;3(2):20–33.
[39] Moradi HJ, Soheilifar S, Nikkhah M, Torkzaban P, Rabienejad N. Effect of implant site preparation by piezoelectric and conventional drilling on autograft cell viability: a clinical trial. J Islam Dent Assoc Iran (JIDAI) 2018;30(2):52–7.

[40] Ma L, Stübinger S, Liu XL, Schneider UA, Lang NP. Healing of osteotomy sites applying either piezosurgery or two conventional saw blades: a pilot study in rabbits. Int Orthop 2013;37(8):1597–603.
[41] Moradi HJ, Arabi SR, Hosseinipanah SM, Solgi G, Rastegarfard N, Farhadian M. Comparison of the effect of three autogenous bone harvesting methods on cell viability in rabbits. J Dent Res Dent Clin Dent Prospects 2017;11(2):73–7.
[42] Alexandre A, Marzia F, Francesco C, Roberta S, Michele B, Alessandro R, Luigi C, Carla P. Structural and ultrastructural analyses of bone regeneration in rabbit cranial osteotomy: piezosurgery versus traditional osteotomes. J Cran Maxillofac Surg 2018;46(1):107–18.